2024 European Control Conference (ECC)
June 25-28, 2024. Stockholm, Sweden

Coalitional model predictive control of building zones temperatures

Filip Vrbanc, Vinko Lešić, Anita Banjac, Mario Vašak
University of Zagreb, Faculty of Electrical Engineering and Computing
Laboratory for Renewable Energy Systems
Zagreb, Croatia
filip.vrbanc@fer.hr, vinko.lesic@fer.hr, anita.banjac@fer.hr, mario.vasak@fer.hr

***Abstract*— This paper deals with the potential benefits of coalition-based modelling and control of building zones heating and cooling to enhance the overall energy efficiency of the building. The paper applies model predictive control for tracking of setpoint temperature in building zones. To tackle the complexity of the model, the approach utilizes semi-physical independent thermal models of building zones and models thermal connections between adjacent zones based on resistive-capacitive analogy. Such coupled models are formed into coalitions and are used in model predictive control of zone temperature. Realistic two 5-day simulations are conducted to compare the performance of the coalitional control. Results indicate that the coalitional control approach reduces energy consumption by up to 14.96% in comparison to decentralized approach of independent model predictive control of each zone while providing consumption increase of 1.38% compared to a centralized floor-based model predictive control. The paper provides evaluation of coalitional control performance based on trade-off between energy savings, user comfort, and computational complexity.**

***Index Terms*— building thermal model, coalitional control, model predictive control, energy efficiency**

I. Introduction

Buildings account for 33% of global energy consumption, with a 2% increase in CO_2 emission during last several years [1]. There is an expressed trend of increase in number of installed air conditioning systems [2]. This trend additionally brings considerable daily peak load periods, resulting in escalated electricity expenses and disrupted energy balance.

Today, emphasis is put on strategies that enhance the thermal performance of buildings and ensure high energy efficiency. This can be achieved by using advanced control technologies such as model predictive control (MPC). Authors in [3] use supervisory MPC for linear time-varying model of building HVAC, which leads to 14.12% comfort improvement. Authors in [4] combine MPC with an artificial neural network for building cooling with adaptive machine-learning-based model of building updated by latest data. With this, the authors report reduction by 58.5% in thermal energy and 36.7% in electric energy. In the [5], physics-based process model is combined with data-driven model to achieve minimisation of modelling effort.

One of the challenges in application of MPC to buildings is the thermal model of zones. The types of mathematical models used in buildings MPC vary from simple to more complex models. Well-accepted method of modelling is resistance-capacitance (RC) method that exploits the analogy with electrical circuits. Despite being physically accurate for large buildings with many zones, models obtained this way are mathematically complex and also require significant expert time to implement the concept [6]. Simple, second-order semi-physical models are representing zones with two thermal masses: a large one with slow dynamics for walls and furniture and a small one with fast dynamics for air in the zone. That enabled the implementation of more sophisticated control systems for holistic building energy management [7].

Faster execution of MPC can be obtained by dividing centralized building model into individual submodels of each zone. This way every zone privacy in terms of chosen setpoint is secured. It is reported in [8] that distributed control achieves 52% lower cost compared to the decentralized control. Moreover, the distributed control provides optimal solution trade-off between model complexity and computational complexity. Coalitional control is a method of distributed control where different parts of a system act as cooperative agents that go through the bargaining process to achieve a joint goal [9].

In this paper, grouping zones in static coalition models based on semi-physical models for each room is proposed. Each combination of joint rooms creates a unique coalition model where every room has its own semi-physical model while adjacent rooms' coupling is represented by auxiliary variables obtained based on RC analogy. A cost related to computational complexity is added to the coalition cost. Moreover, a trade-off between energy savings, user comfort, and computational complexity is achieved, which determines if coalitional control is favorable for a specific scenario compared to individual control. Finally, it provides additional flexibility in the optimization of the computational and communication requirements [10].

This paper is organized as follows. In Section II, modelling approach is outlined. In Section III, the case study pilot is described. Moreover, the coalition formation approach is explained in detail. Mathematical derivation is given, together with the case study application. In section IV, a control algorithm for the noted coalition model is provided. Section V gives a realistic 5-day simulation of coalitional, decentralized and centralized control. Also, obtained results are compared. Section VI concludes the paper.

This work has been supported in part by Croatian Science Foundation under the project No. UIP-2020-02-9636 (project DECIDE - Distributed Control for Dynamic Energy Management of Complex Systems in Smart Cities).

II. BUILDING THERMAL MODEL

This paper considers the 9th floor of the skyscraper building of University of Zagreb Faculty of Electrical Engineering and Computing. The thermal model of the considered floor is obtained by using semi-physical modelling, briefly described in this section. In the paper, three different model configurations are considered: i) decentralized building zone models, ii) centralized building model, and iii) coalitional building model. Indoor temperature outputs of the model are related to 23 offices.

The independent semi-physical model of a single zone is initially proposed in [11]. For simplicity and due to the fact that temperature distribution was uniformly distributed for the considered case-study the heat transmission between adjacent zones was ignored. Model parameters are identified by using unscented Kalman filter and real building operational data. Finally, a simple mathematical model for each of the 23 offices is obtained, suitable for MPC. The obtained models are independent and controlled by individual zone MPC. The neglected dynamics of zones heat exchange coupling is justified for similar heating conditions of the zones. The aim of this paper is to exploit the energy savings in highly-dynamical, heterogeneous scenarios, with noticeable temperature differences between zones. In the sequel, modified model that combines several independent semi-physical models into a coalition is derived and explained.

A. Coalitional building model

Connecting adjacent zones based on coalitional zone modellling gives zones opportunities to share data and achieve higher energy efficiency. Only adjacent zones can join a coalition which means every zone in a coalition needs to have at least one adjacent wall with at least one of the zones in the same coalition. To account the coupling between adjacent zones mathematical model from [11] is extended by the inclusion of coupling derived through the RC modelling approach. This way, the coalitional building model is a compromise and combination of both approaches, RC and semi-physical. The following model shows a coalition of two exemplary adjacent zones:

$$C_1^{\mathrm{A}}\dot{T}_1^{\mathrm{A}} = \frac{1}{R_{\mathrm{out}}^{\mathrm{A}}}(T_{\mathrm{out}} - T_1^{\mathrm{A}}) + \frac{1}{R^{\mathrm{A}}}(T_2^{\mathrm{A}} - T_1^{\mathrm{A}}) + \epsilon_1^{\mathrm{A}} I^{\mathrm{dir}} + \epsilon_2^{\mathrm{A}} I^{\mathrm{diff}} + P_{\mathrm{t}}^{\mathrm{A}} + \frac{1}{R_{\mathrm{w}}^{\mathrm{A}}}(T_{\mathrm{w}}^{\mathrm{A}} - T_1^{\mathrm{A}}), \quad (1)$$

$$C_2^{\mathrm{A}}\dot{T}_2^{\mathrm{A}} = \frac{1}{R^{\mathrm{A}}}(T_1^{\mathrm{A}} - T_2^{\mathrm{A}}), \quad (2)$$

$$C_1^{\mathrm{B}}\dot{T}_1^{\mathrm{B}} = \frac{1}{R_{\mathrm{out}}^{\mathrm{B}}}(T_{\mathrm{out}} - T_1^{\mathrm{B}}) + \frac{1}{R^{\mathrm{B}}}(T_2^{\mathrm{B}} - T_1^{\mathrm{B}}) + \epsilon_1^{\mathrm{B}} I^{\mathrm{dir}} + \epsilon_2^{\mathrm{B}} I^{\mathrm{diff}} + P_{\mathrm{t}}^{\mathrm{B}} + \frac{1}{R_{w}^{\mathrm{B}}}(T_{\mathrm{w}}^{\mathrm{B}} - T_1^{\mathrm{B}}), \quad (3)$$

$$C_2^{\mathrm{B}}\dot{T}_2^{\mathrm{B}} = \frac{1}{R^{\mathrm{B}}}(T_1^{\mathrm{B}} - T_2^{\mathrm{B}}), \quad (4)$$

$$C_{\mathrm{w}}^{\mathrm{A}}\dot{T}_{\mathrm{w}}^{\mathrm{A}} = -\left(\frac{1}{R_{\mathrm{w}}^{\mathrm{A}}} + \frac{1}{R_{\mathrm{w}}^{\mathrm{AB}}}\right)T_w^{\mathrm{A}} + \frac{1}{R_{w}^{\mathrm{AB}}}T_{\mathrm{w}}^{\mathrm{B}} + \frac{1}{R_{\mathrm{w}}^{\mathrm{A}}}T_1^{\mathrm{A}}, \quad (5)$$

$$C_{\mathrm{w}}^{\mathrm{B}}\dot{T}_{\mathrm{w}}^{\mathrm{B}} = -\left(\frac{1}{R_{\mathrm{w}}^{\mathrm{B}}} + \frac{1}{R_{\mathrm{w}}^{\mathrm{AB}}}\right)T_{\mathrm{w}}^{\mathrm{B}} + \frac{1}{R_{\mathrm{w}}^{\mathrm{AB}}}T_{\mathrm{w}}^{\mathrm{A}} + \frac{1}{R_{\mathrm{w}}^{\mathrm{B}}}T_1^{\mathrm{B}}, \quad (6)$$

where the superscripts A and B denote variables and coefficients of the first zone and second zone, respectively. Equations (1)-(4) represent inner dynamics of the zones. Variables T_1 and T_2 are temperatures of air (fast dynamics) and solid zone parts excluding the joint wall (slow dynamics), respectively. The C_1 is air capacity, while C_2 is larger, solid zone parts capacity. Parameter R represents thermal resistance between zone air and furniture. Outside temperature is denoted with T_{out}, while R_{out} represents thermal resistance between outside and zone air. P_{t} represents a thermal load that directly influences the thermal conditions within the zone. The zone is further influenced by two distinct types of solar irradiance: diffuse solar irradiance (I^{diff}) and direct solar irradiance (I^{dir}). These irradiance components interact with the exterior surface of the zone, impacting its thermal dynamics through the corresponding solar transmittance parameters, ϵ_1 and ϵ_2.

Last part of the first equation in (1) includes variable $T_{\mathrm{w}}^{\mathrm{A}}$ which stands for the temperature of the adjacent wall face in zone A. The $R_{\mathrm{w}}^{\mathrm{A}}$ represents thermal resistance between air temperature in zone A and the adjacent wall surface in zone A. Analogously, last part of (3) includes variable $T_{\mathrm{w}}^{\mathrm{B}}$ which stands for the temperature of the adjacent wall face in zone B. The $R_{\mathrm{w}}^{\mathrm{B}}$ represents thermal resistance between air temperature in zone B and the wall surface in zone B. Equations (5) and (6) describe heat transfer through the adjacent wall. Parameters $C_{\mathrm{w}}^{\mathrm{A}}$ and $C_{\mathrm{w}}^{\mathrm{B}}$ outline thermal capacity of each side of the wall, while $R_{\mathrm{w}}^{\mathrm{AB}}$ represents thermal resistance between two sides of the wall.

Adjacent walls are modelled with two equations, where each variable represents the temperature on one side of the wall. Rooms interconnection through halls and toilets is neglected for the purpose of this work since temperature references in halls and toilets are not controlled in this case study.

III. CASE-STUDY

The scheme of the considered building floor is given in Fig. 1. Blue-coloured rooms represent block I, green block II, while yellow represent block III. There are two extremes - one where each room is its own coalition and it is equal to the decentralized model; and the other where the whole block creates a joint coalition which counts as three centralized models. Two rooms can be together as part of a coalition only if all the other rooms between them exist in the same coalition, e.g. C09-01 and C9-02a can create their own coalition model since they are adjacent, but a condition for C09-01 and C09-04 to create a coalition is to add C09-02a to it.

The number of possible coalitions in each block depends on the number of zones in the block and it is given as follows:

$$\text{no. of coalitions} = \sum_{i=1}^{\text{no. of zones}} i. \quad (7)$$

Therefore, there are 66 possible coalitions in Block I, 10 in Block II, and 36 in Block III. For the sake of simplicity the

Fig. 1. Tthe 9th floor of FER building- blocks distribution

paper considers exemplary topology of a static coalition that includes: C9-01, C9-02a and C9-04. All other zones from Block I form a separate coalition. However, in future work, coalitions layout will be evaluated in each time step. The discrete-time coalitional model of the considered coalition is written in state-space form as follows:

$$x(k+1) = Ax(k) + B_{\mathrm{u}}u(k) + B_{\mathrm{d}}d(k), \quad k \in \mathbb{Z}, \tag{8}$$

where A, B_{u}, and B_{d} are discrete model matrices with a sampling time of 15 minutes obtained based on the approach presented by equations (1)-(4) and discretized using ZOH discretization method. Vector x contains air temperatures, slow dynamics temperatures and adjacent wall's faces temperatures. Vector u includes thermal power input, while vector d includes outside temperature and direct and diffuse solar irradiance.

Furthermore, dimension of model matrix A of each coalition depends on number of included rooms. Each room semi-physical model contains tewo states, while the number of model states is increased by two, for a pair of adjacent zones. In general case, the following equation for number of model states n_x is given:

$$n_x = 2n + 2(n-1), \tag{9}$$

where n is a number of involved rooms. For the considered case-study of coalitional model with three adjacent zones vector x contains 10 states:

$$x = [T_1^{\mathrm{A}},\, T_2^{\mathrm{A}},\, T_1^{\mathrm{B}},\, T_2^{\mathrm{B}},\, T_1^{\mathrm{C}},\, T_2^{\mathrm{C}},\, T_{\mathrm{w}}^{\mathrm{A}},\, T_{\mathrm{w}}^{\mathrm{B1}},\, T_{\mathrm{w}}^{\mathrm{B2}},\, T_{\mathrm{w}}^{\mathrm{C}}]^T, \tag{10}$$

where superscripts A, B, and C correspond to C9-01, C9-02a, and C9-04, respectively. Variable $T_{\mathrm{w}}^{\mathrm{B1}}$ represents temperature of the adjacent wall face in C9-02a closed to C9-01, while variable $T_{\mathrm{w}}^{\mathrm{B2}}$ represents temperature of the adjacent wall face in C9-02a closed to C9-04. Therefore, matrix A for the considered case study coalition is given:

$$\begin{bmatrix}
a_1 & a_2 & 0 & 0 & 0 & 0 & a_3 & 0 & 0 & 0 \\
a_4 & a_5 & 0 & 0 & 0 & 0 & 0 & 0 & 0 & 0 \\
0 & 0 & a_6 & a_7 & 0 & 0 & 0 & a_8 & a_9 & 0 \\
0 & 0 & a_{10} & a_{11} & 0 & 0 & 0 & 0 & 0 & 0 \\
0 & 0 & 0 & 0 & a_{12} & a_{13} & 0 & 0 & 0 & a_{14} \\
0 & 0 & 0 & 0 & a_{15} & a_{16} & 0 & 0 & 0 & 0 \\
a_{17} & 0 & 0 & 0 & 0 & 0 & a_{18} & a_{19} & 0 & 0 \\
0 & 0 & a_{20} & 0 & 0 & 0 & a_{21} & a_{22} & 0 & 0 \\
0 & 0 & a_{23} & 0 & 0 & 0 & 0 & 0 & a_{24} & a_{25} \\
0 & 0 & 0 & 0 & a_{26} & 0 & 0 & 0 & a_{27} & a_{28}
\end{bmatrix}. \tag{11}$$

Parameters a_1, a_2, a_4, and a_5 are related to semi-physical model of C9-01. Parameters a_6, a_7, a_{10}, and a_{11} are related to semi-physical model of C9-02a. Parameters a_{12}, a_{13}, a_{15}, and a_{16} are related to semi-physical model of C9-04. Parameters a_3 and a_{17} show connection of C9-01 with bordering wall, while a_{20} and a_8 show connection of C9-02a to the same wall. These two wall variables are related through parameters a_{18}, a_{19}, a_{21}, and a_{22}. Analogously, parameters a_9 and a_{23} show relation between room C9-02a and wall adjacent to C9-04, while relation between C9-04 and wall is given by parameters a_{14} and a_{26}. These two parameters are interconnected by a_{24}, a_{25}, a_{27}, and a_{28}. Values of each parameter included in matrix A of the noted coalition are given in Table 1. Size of vector u is 3, which means it contains one input for each room in coalition. Parameters noted with b correspond to C9-01, parameters noted with c correspond to C9-02a, while parameters noted with d correspond to C9-04. Values of parameters are given in Table

TABLE I

MATRICES PARAMETERS

Parameter	Value	Parameter	Value
a_1	0.5134	b_1	0.0185
a_2	0.4679	b_2	0.0015
a_3	0.0038	b_3	0.0030
a_4	0.0469	b_4	0.3835
a_5	0.9525	b_5	$6.7163 \cdot 10^{-4}$
a_6	0.5459	b_6	$5.5165 \cdot 10^{-5}$
a_7	0.4320	b_7	$1.0922 \cdot 10^{-4}$
a_8	0.0082	b_8	0.0139
a_9	0.0048	c_1	0.0221
a_{10}	0.0403	c_2	0.0024
a_{11}	0.9590	c_3	0.0032
a_{12}	0.5194	c_4	0.4804
a_{13}	0.4621	c_5	$6.6186 \cdot 10^{-4}$
a_{14}	0.0031	c_6	$7.0526 \cdot 10^{-5}$
a_{15}	0.0475	c_7	$9.6334 \cdot 10^{-5}$
a_{16}	0.9518	c_8	0.0144
a_{17}	0.0034	d_1	0.0185
a_{18}	0.9943	d_2	0.0015
a_{19}	0.0010	d_3	0.0036
a_{20}	0.0035	d_4	0.8217
a_{21}	0.0010	d_5	$6.7591 \cdot 10^{-4}$
a_{22}	0.9943	d_6	$5.3128 \cdot 10^{-5}$
a_{23}	$8.9164 \cdot 10^{-5}$	d_7	$1.3046 \cdot 10^{-4}$
a_{24}	0.9997	d_8	0.0301
a_{25}	$2.2857 \cdot 10^{-4}$		
a_{26}	$8.7085 \cdot 10^{-5}$		
a_{27}	$2.2857 \cdot 10^{-4}$		
a_{28}	0.9997		

1. Matrix B for the same coalition is:

$$\begin{bmatrix} b_1 & b_2 & b_3 & b_4 & 0 & 0 & 0 & 0 & 0 & 0 & 0 & 0 \\ b_5 & b_6 & b_7 & b_8 & 0 & 0 & 0 & 0 & 0 & 0 & 0 & 0 \\ 0 & 0 & 0 & 0 & c_1 & c_2 & c_3 & c_4 & 0 & 0 & 0 & 0 \\ 0 & 0 & 0 & 0 & c_5 & c_6 & c_7 & c_8 & 0 & 0 & 0 & 0 \\ 0 & 0 & 0 & 0 & 0 & 0 & 0 & 0 & d_1 & d_2 & d_3 & d_4 \\ 0 & 0 & 0 & 0 & 0 & 0 & 0 & 0 & d_5 & d_6 & d_7 & d_8 \\ 0 & 0 & 0 & 0 & 0 & 0 & 0 & 0 & 0 & 0 & 0 & 0 \\ 0 & 0 & 0 & 0 & 0 & 0 & 0 & 0 & 0 & 0 & 0 & 0 \\ 0 & 0 & 0 & 0 & 0 & 0 & 0 & 0 & 0 & 0 & 0 & 0 \\ 0 & 0 & 0 & 0 & 0 & 0 & 0 & 0 & 0 & 0 & 0 & 0 \end{bmatrix}. \quad (12)$$

IV. MODEL PREDICTIVE CONTROL

This section focuses on the utilization of the derived model for MPC. The control problem algorithm is implemented in a receding fashion and it is coded in Matlab. Construction of matrices over the horizon is performed by using Yalmip toolbox [12]. The solution of optimisation problem is obtained by IBM CPLEX solver [13]. A prediction horizon of 5 hours is chosen together with a sampling time of 15 minutes as proven adequate to capture the relevant dynamics for such high-level temperature control. Each thermal power is constrained by:

$$u_{\mathrm{i,min}} \leq u_i \leq u_{\mathrm{i,max}}, \quad (13)$$

where i represents corresponding zone, while $u_{\max}$ and $u_{\min}$ are maximum heating and maximum cooling power, respectively. Global power constraints are not considered in this paper. During periods when reference tracking is active, each zone temperature is soft constrained by [14]:

$$w_i - \Delta - \delta_i \leq y_i \leq w_i + \Delta + \delta_i, \quad (14)$$

where y_i represents air temperature of the corresponding zone, while w_i stands for zone temperature setpoint. Parameter Δ allows zone temperature to deviate from setpoint within predefined limits and it is set to 0.5 $^\circ C$. In addition, δ_i represents slack variable of each zone. Slack variables allow temperature deviation outside predefined limits to ensure feasible implementation, despite being highly penalized. Moreover, temperature is constrained by building protect limits:

$$y_{\min} - \Delta - \sigma_i \leq y_i \leq y_{\max} + \Delta + \sigma_i, \quad (15)$$

where $y_{\max}$ and $y_{\min}$ are maximal and minimal allowed temperature, respectively. The σ_i stands for deviation from building protect limits.

Cost function J, where $J_{k=-1}$ is defined as zero, for each zone of the problem is a linear quadratic function in the form of a reference w tracking problem:

$$\begin{aligned} J_k =& J_{k-1} + (y_{k+1} - w_{k+1})^T Q (y_{k+1} - w_{k+1}) \\ &+ u_k^T R u_k + \delta_{k+1}^T G_1 \delta_{k+1} + \sigma_{k+1}^T G_2 \sigma_{k+1} \\ & k \in [0, N-1], \end{aligned} \quad (16)$$

where $Q, G_1 = 0$ for non-working hours. Variable y stands for zone air temperature and N is time horizon. During working hours cost function takes into account difference between indoor air temperature and the selected setpoint, energy consumption, deviation of the zone comfort constraint, and deviation from building limits. During non-working hours, only energy minimisation criterion is active. Balanced trade-off between reference tracking and energy savings is made by choosing matrices R, Q, and G. Matrix R is set to be identity matrix. Matrix Q is calculated by:

$$Q = \gamma R F, \quad (17)$$

since cost of energy minimisation is expressed in watts, while tracking criterion is temperature. Parameter γ is a weighting factor for significance of setpoint tracking over energy consumption as defined in [14]. Matrix F ensures unit conversion and is derived in the sequel. Discrete model in state-space form (8) is reformulated to:

$$y = CAx + CB_u u + CB_d d, \quad (18)$$

where y represents air temperature from (16), matrix C expresses relation between model outputs and all model states, while matrix B_u represent part of matrix B related to power inputs and matrix B_d is part related to disturbances. Vector d is vector that includes outside temperature and solar irradiances. From (18) variable u is calculated by:

$$u = C^{-1} B_u^{-1} (y - CAx - CB_d d). \quad (19)$$

Considering quadratic cost function u^2 is calculated by:

$$\begin{aligned} u^2 = (CB_u)^{-2} [& y^2 + (CAx)^2 + (CB_d d)^2 \\ & - 2yCAx + 2CAxCB_d d - 2CB_d dy]. \end{aligned} \quad (20)$$

Therefore, sensitivity of quadratic energy consumption to the quadratic zone temperature is calculated by:

$$\frac{\partial u^2}{\partial y^2} = (CB_u)^{-2} = F. \tag{21}$$

Complexity of the quadratic problem is expressed as a cubic polynomial function [15]:

$$O(n) = Kn^3N, \tag{22}$$

where K stands for trade-off between energy savings and system complexity. The n represents the number of problem state-space variables.

Furthermore, total cost function of coalition (J_{tot}) sums costs off all zones extended on time horizon:

$$J_{\text{tot}} = \sum_{i=1}^{N_z} \sum_{k=0}^{N-1} J_k + Kn^3N, \tag{23}$$

where N_z stands for number of zones in the coalition.

V. Simulation results

The realistic simulation is performed for two working weeks in January and February 2023 by using the continuous model. The disturbances are shown in Fig. 2 for January. We assume that disturbances are predicted and known in advance, providing the deterministic scenario. Graph data show that during January week, Wednesday, Thursday, and Friday achieve a higher level of solar irradiance. Direct irradiance for the north side of the building is equal to zero, so the graph shows only direct irradiance for the south side. However, the diffuse irradiance of both sides of the building is the same. The setpoint pattern is selected to be the same for every day. During working hours, from 08:00 to 16:00 temperature reference ('SP') of 22 $^\circ C$ is chosen. On the other hand, during off-work setpoint is neglected. The sampling time is 15 minutes, and MPC parameter γ is set to be 1. Parameter K is set to 0.0077 and time horizon is 6 hours. Only heating is enabled while using HVAC for cooling is disabled since it is a winter month. Three simulations of the case study are performed.

In the first one, offices C9-01, C9-02a, and C9-04 altogether join the coalition ('Col-MPC' in legend), while another part of block I (offices from C9-05 to C9-12) form a separate coalition. Moreover, the whole block II is unique coalition, as it is block III. Second case implies C9-01, C9-02a, and C9-04 are three independent coalitions so that each coalition includes only one office ('I-MPC' in legend). The other part of the floor, is structured in the same way as in the first case. Last case contains one large coalition formed by all block I zones, while blocks II and III form their separate coalitions ('C-control' in legend). The MPC control is implemented in a moving horizon fashion where 5 hours predictions are taken into account. After each calculation, the current solution is taken, so obtained thermal power is used for the next 15 minutes. Simulation is performed using centralized model as a physically trustworthy model considered to show behaviour approximately the same as the real system. After each time period, measurements of room air temperature obtained by the centralized model are delivered to the MPC, which uses it as a new initial condition. This way the simulation of a real-time scenario is executed.

Figure 3 shows a comparison of room temperature between the three approaches. It can be seen that temperature response of coalitional control is much closer to the centralized control response, in comparison to the individual control. During January, zone C9-02a is overheated because of the heat conducted from adjacent zones (C9-01 and C9-04). Coalitional and centralized control react better in comparison to individual control because they take heat exchange through adjacent walls into account. During February, room temperature exceeds setpoint due to higher level of solar irradiances and disability to use cooling. Root mean square error (RMSE) of reference tracking for coalitional control is 9.56% (January) and 3.12% (February) lower compared to decentralized control

Figures 4 shows that for all three rooms, energy consumption is lower when they are part of the coalition. Due to warmer weather, usage of thermal power is lower during February. Daily energy consumption for those three offices in January is 121.17 kWh in the case of coalitional MPC, 124.38 kWh in the case of decentralized control, and 120.79 kWh in the case of centralized MPC, which leads to energy savings of 2.5%. Despite consuming 0.3% more energy than centralized control, additional benefit of coalitional MPC is also high user privacy since data is not shared outside of coalition zones. Furthermore, during February, energy savings of coalitional control are 14.96% compared to decentralized control, while consumption increase compared to centralized control is 1.38%.

The drawback of coalitional control compared to decentralized is higher system order which leads to slower computation. In this case, coalitional model contains ten state-space variables, while each one of the individual zone models contains only two. Therefore, in January, energy savings are 3.21 kWh, and the total cost of coalitional control is lower compared to decentralized control by 36. On the other hand, during February, energy savings are only 1.46 kWh, while the total cost of coalitional control is higher by 20. Therefore, by computing total cost by (23), it can be decided whether coalitional control improves system energy savings and user comfort high enough. Despite being computationally more complex, in some scenarios (e.g. January) coalitional control is favourable, while in others (e.g. February) it is not.

VI. Conclusion

This paper explains a coalition modelling approach combining RC modelling approach and semi-physical modelling approach. The research focuses on a case study of the 9th floor of the Faculty of Electrical Engineering and Computing in Zagreb. By developing coalitions of adjacent rooms, data sharing and joint control opportunities are leveraged to achieve higher energy efficiency. The result of the simulation indicates that the proposed coalition control approach

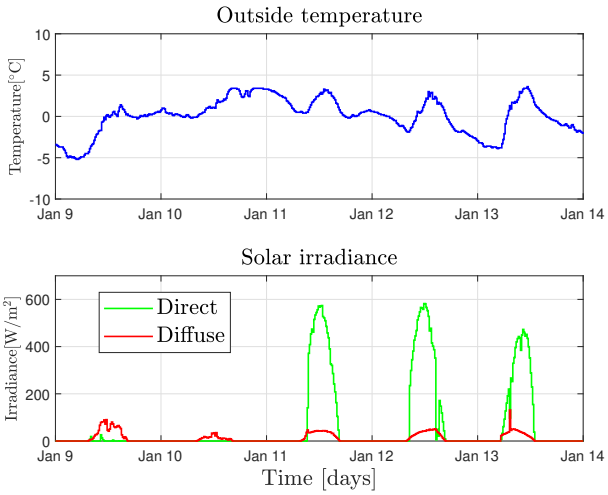

Fig. 2. Disturbances - January

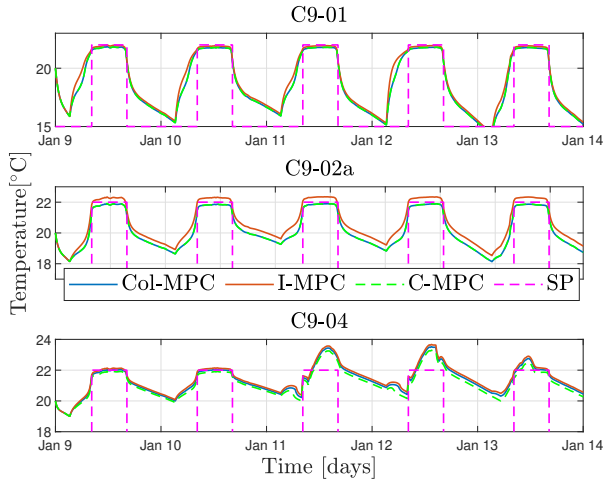

Fig. 3. Temperature comparison - January

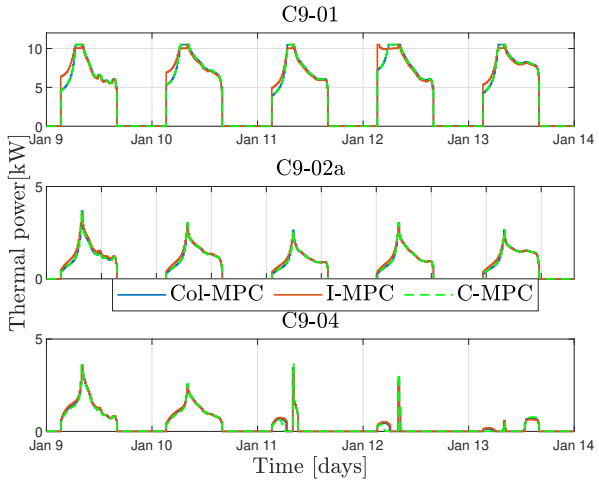

Fig. 4. Thermal power comparison - January

achieves higher energy efficiency compared to decentralized control. The coalition control leads to significant energy savings, reducing energy consumption for the coalition of offices in the case study. Furthermore, the coalitional model has the advantage compared to the individual one, especially during periods with high temperature deviation between them. Moreover, by adding computational complexity cost, it is possible to be make a decision between coalitional and individual control. The algorithm which includes that decision-maker in real-time is a base for dynamic coalitional control.

REFERENCES

[1] Quarterly greenhouse gas emissions in the EU, 4th quarter 2022., Eurostat

[2] Directive of the european parliament and of the council on the energy performance of buildings, European commission, 2021.

[3] S. Promchaiwattana and D. Banjerdpongchai, "Design of Supervisory Model Predictive Control for Building HVAC System Subject to Time-Varying Operating Points," 2022 22nd International Conference on Control, Automation and Systems (ICCAS), Jeju, Korea, Republic of, 2022, pp. 1404-1409, doi: 10.23919/ICCAS55662.2022.10003843.

[4] Shiyu Yang, Man Pun Wan, Wanyu Chen, Bing Feng Ng, Swapnil Dubey, Model predictive control with adaptive machine-learning-based model for building energy efficiency and comfort optimization, Applied Energy, Volume 271, 2020, 115147, ISSN 0306-2619, https://doi.org/10.1016/j.apenergy.2020.115147.

[5] P. Stoffel, C. Löffler, S. Eser, A. Kümpel and D. Müller, "Combining Data-driven and Physics-based Process Models for Hybrid Model Predictive Control of Building Energy Systems," 2022 30th Mediterranean Conference on Control and Automation (MED), Vouliagmeni, Greece, 2022, pp. 121-126, doi: 10.1109/MED54222.2022.9837277.

[6] D. Sturzenegger, D. Gyalistras, M. Morari and R. S. Smith, "Model Predictive Climate Control of a Swiss Office Building: Implementation, Results, and Cost–Benefit Analysis," in IEEE Transactions on Control Systems Technology, vol. 24, no. 1, pp. 1-12, Jan. 2016, doi: 10.1109/TCST.2015.2415411.

[7] A. Banjac, H. Novak, M. Vašak, "Implementation of model predictive indoor climate control for hierarchical building energy management", Control Engineering Practice, Volume 136, 2023, 105536, ISSN 0967-0661, https://doi.org/10.1016/j.conengprac.2023.105536.

[8] F. Vrbanc and V. Lešić, "Distributed Optimal Heating Control of Building Zones," 2021 23rd International Conference on Process Control (PC), Strbske Pleso, Slovakia, pp. 78-83, 2021.

[9] F. Fele, E. Debada, J. M. Maestre and E. F. Camacho, "Coalitional Control for Self-Organizing Agents," in IEEE Transactions on Automatic Control, vol. 63, no. 9, 2018.

[10] F. Fele, J. M. Maestre and E. F. Camacho, "Coalitional Control: Cooperative Game Theory and Control," in IEEE Control Systems Magazine, vol. 37, no. 1, pp. 53-69, 2017.

[11] A. Martinčević and M. Vašak, "Constrained Kalman Filter for Identification of Semiphysical Building Thermal Models," in IEEE Transactions on Control Systems Technology, vol. 28, no. 6, pp. 2697-2704, 2020.

[12] J. Lofberg, "YALMIP : a toolbox for modeling and optimization in MATLAB," 2004 IEEE International Conference on Robotics and Automation, Taipei, Taiwan, 2004, pp. 284-289

[13] IBM ILOG CPLEX, "Optimization Studio Getting Started with CPLEX for MATLAB"

[14] A. Martinčević, M. Vašak and V. Lešić, "Model predictive control for energy-saving and comfortable temperature control in buildings," 2016 24th Mediterranean Conference on Control and Automation (MED), Athens, Greece, 2016, pp. 298-303

[15] Ye, Y., Tse, E. An extension of Karmarkar's projective algorithm for convex quadratic programming. Mathematical Programming 44, 157–179 (1989).